Research Square

Preprints are preliminary reports that have not undergone peer review.
They should not be considered conclusive, used to inform clinical practice,
or referenced by the media as validated information.

Diagnosing Spatial Disparities in Urban Flood Burden through Hydro- Environmental Normalization in Jakarta, Indonesia

Rifky Husaini
IPB University
Perdinan Perdinan
perdinan@apps.ipb.ac.id

IPB University
Novindra Novindra
IPB University

Research Article

Keywords: urban flooding, flood burden, hydro-environmental normalization, observed-expected diagnostics, geospatial monitoring, spatial disparities, Jakarta

Posted Date: August 11th, 2026

DOI: https://doi.org/10.21203/rs.3.rs-10560084/v1

License: This work is licensed under a Creative Commons Attribution 4.0 International License.
Read Full License

Additional Declarations: No competing interests reported.

Diagnosing Spatial Disparities in Urban Flood Burden through Hydro-Environmental Normalization in Jakarta, Indonesia

Rifky Husaini[1], Perdinan[1*], Novindra[2]

[1] Department of Geophysics and Meteorology, IPB University, Dramaga Campus, Bogor, West Java 16680 Indonesia

[2] Department of Resources and Environmental Economics, IPB University, Dramaga Campus, Bogor, West Java 16680 Indonesia

[*] Corresponding author: perdinan@apps.ipb.ac.id

Abstract

Urban flood assessment identifies where hazards, exposure, or vulnerability are greatest, but it less often asks whether realized flood burden is unusually high or low relative to the environmental conditions under which it occurs. This study develops Hazard-Normalized Flood Burden Deviation (HNFBDev), an observed–expected geospatial diagnostic that identifies where urban flood burden is higher or lower than expected under represented hydro-environmental conditions. Using Jakarta as a case study, the framework combines hydro-environmental forcing, Sentinel-1 flood observations, population exposure, environmental expectation modelling, and spatial diagnostics. The hydro-environmental baseline represents inland and coastal conditions, while the population-exposure-weighted flood-burden proxy captures the intersection of flood observations and exposed population. Environmentally expected burden is estimated from the forcing baseline, and HNFBDev is derived as the standardized deviation between observed and expected burden. The results show that compound hydro-environmental forcing was significantly associated with observed burden and explained only part of its spatial variation. The HNFBDev surface identified locations where observed burden was higher or lower than expected under comparable conditions, with significant spatial clustering and robustness under alternative weighting assumptions. These findings demonstrate that flood-burden disparities cannot be interpreted from hazard, exposure, or observed inundation alone. HNFBDev provides a transferable observed–expected geospatial diagnostic, subject to local calibration and validation, for identifying places where flood outcomes warrant hydraulic, infrastructure, institutional, and local verification. It should be interpreted as a screening and prioritization tool, not as a direct measure of adaptation performance, resilience, governance quality, infrastructure effectiveness, social vulnerability, flood depth, or causal mechanisms.

Keywords: urban flooding; flood burden; hydro-environmental normalization; observed-expected diagnostics; geospatial monitoring; spatial disparities; Jakarta

1. Introduction

Urban flooding increasingly emerges from interacting with hydro-environmental and land-surface processes rather than from a single flood-generating mechanism. In coastal and deltaic cities, intense rainfall, river discharge, tidal or storm-surge effects, land subsidence, low-lying terrain, impervious-surface expansion, and constrained drainage systems may coincide or occur in close sequence, producing flood outcomes that are difficult to infer from one driver alone. Recent compound-flood literature emphasizes precisely this interaction among fluvial, pluvial, coastal, groundwater, and antecedent environmental conditions, particularly in coastal-estuarine settings where drainage and marine processes are tightly connected [1], [2], [3], [4]. Jakarta illustrates this complexity clearly. Process-based modelling has shown that storm-driven increases in coastal water levels can obstruct river drainage and elevate water levels around river outlets, while long-term sea-level rise and land subsidence amplify future coastal-flood exposure in the northern parts of the city [5]. Similar concerns have been raised across Asian megadeltas, where coastal flooding reflects interactions among global climate pressures, local subsidence, land-use change, and human modification of deltaic systems [6].

Urban flood assessment has advanced substantially through hydrodynamic modelling, flood-susceptibility mapping, remote sensing, exposure analysis, and vulnerability assessment. Hydrodynamic and susceptibility approaches have improved the identification of locations where flood hazards are likely to occur, while satellite observations now allow inundation to be mapped more consistently across large areas and repeated events. Population-exposure studies have further demonstrated the value of combining flood footprints with gridded population data to estimate who may be affected, rather than interpreting inundated area alone [7], [8], [9]. At the same time, flood-impact and damage research has long noted that estimating consequences remains more uncertain than mapping physical inundation, because losses and burdens depend on how floodwater intersects with people, assets, protection systems, and local response capacity [10]. These advances have substantially improved the characterization of flood hazards, exposure, and impacts, but they do not explicitly distinguish whether realized urban flood burden is disproportionately high or low relative to the hydro-environmental conditions under which it occurs.

This distinction matters because similar flood-generating conditions do not necessarily produce similar realized urban flood burdens. Differences in population concentration, urban morphology, drainage connectivity, flood-control infrastructure, institutional arrangements, preparedness, and social vulnerability can alter how physical flooding is translated into experienced consequences. Global and national studies have shown that flood exposure and flood risk are socially and spatially uneven, while evidence from vulnerability and adaptation research indicates that flood impacts may decline, persist, or shift depending on risk-management capacity and the constraints faced by exposed communities [11], [12], [13], [14]. Recent neighbourhood-level analyses also show that urban flood exposure may be patterned along socioeconomic gradients, reinforcing the need to examine flood burden as a spatially differentiated outcome rather than a simple

expression of hazard intensity [15]. For this reason, an area with a higher observed burden is not necessarily poorly managed, and an area with a lower observed burden is not necessarily resilient. Both interpretations require a benchmark that first accounts for the environmental conditions under which the observed burden is realized.

Observed-expected diagnostic reasoning offers one way to construct such a benchmark. In ecological and water-quality assessment, reference-condition approaches compare observed system conditions with conditions expected under comparable environmental settings, thereby allowing departures from expectation to be interpreted more consistently across heterogeneous landscapes [16], [17]. Mazor et al. [18] similarly emphasize the importance of designing indices whose meaning remains comparable across different environmental contexts, while Hamalainen et al. [19] caution that observed-expected ratios and residuals can become biased when expectation-dependent variance is not handled carefully. These lessons are directly relevant to urban flood assessment. An observed–expected flood-burden diagnostic should not merely rank places by observed inundation or exposure; it should ask whether realized urban flood burden is higher or lower than would be expected given comparable hydro-environmental conditions. Such a diagnostic must also be statistically cautious, because residual patterns may reflect unrepresented hydro-environmental or urban processes, model specification, spatial dependence, measurement uncertainty, or genuine outcome disparities.

Despite these conceptual foundations, urban flood studies have rarely implemented an observed–expected geospatial diagnostic that integrates a population-exposure-weighted observed flood-burden proxy derived from satellite observations, gridded population exposure, hydro-environmental expectation modelling, spatial diagnostics, and robustness assessment within a single analytical framework [7]. Conventional hazard and susceptibility maps help identify where flood-prone conditions exist, while exposure and vulnerability assessments identify who or what may be affected. What remains less developed is a spatial diagnostic that separates represented hydro-environmental forcing from realized urban flood burden and then examines whether the remaining deviations form coherent geographic patterns. This gap is especially relevant for urban climate and smart-city applications, where geospatial monitoring is expected not only to map hazards but also to support evidence-based prioritization, follow-up investigation, and repeated assessment of risk-reduction actions. The resulting diagnostic is intended to complement, not replace, hydrodynamic models, vulnerability assessments, or infrastructure audits.

Against this background, this study develops and demonstrates the Hazard-Normalized Flood Burden Deviation, or HNFBDev, as an observed–expected geospatial diagnostic for identifying where population-exposure-weighted urban flood-burden proxy is higher or lower than expected underrepresented hydro-environmental conditions. The overall goal is to identify spatial disparities in urban flood burden after accounting for differences in hydro-environmental forcing. Using Jakarta as a case study, the analysis pursues three objectives: first, to construct a spatially consistent hydro-environmental forcing baseline and a population-exposure-weighted observed flood-burden proxy derived from satellite observations; second, to estimate environmentally expected flood burden and derive

HNFBDev from the standardized deviation observed and environmentally expected burden; and third, to examine whether the resulting deviations are spatially organized and robust across alternative analytical assumptions. The study asks how hydro-environmental forcing relates to multiyear population-exposure-weighted observed burden proxy, where observed burden exceeds or falls below environmental expectations, whether these deviations form statistically significant clusters, and how stable the resulting spatial patterns remain under the alternative analytical specifications evaluated in this study. These objectives are based on the expectation that hydro-environmental forcing explains an important component of population-exposure-weighted burden proxy, while meaningful observed–expected deviations remain after environmental normalization and exhibit coherent spatial organization. By addressing these questions, the paper contributes an observed–expected geospatial diagnostic framework that provides a reproducible screening layer for geospatial monitoring of relative flood-burden disparities: HNFBDev identifies locations where further investigation is warranted, but it does not by itself measure adaptation success, resilience, governance quality, or infrastructure performance.

2. Materials and methods

2.1 Study design, study area, and data

This study applied a geospatial observed-expected diagnostic design to evaluate where population-exposure-weighted urban flood burden is higher or lower than expected under represented conditions, thereby providing a reproducible screening layer for targeted investigation and climate-resilient urban planning. The analysis was organized at the *kelurahan* (urban-village) level, covering 261 administrative units across the Special Capital Region of Jakarta. This spatial unit provides a practical compromise between local detail and data consistency: it is fine enough to preserve intra-urban variation in environmental conditions and flood burden, while still allowing satellite-derived flood observations, population surfaces, and hydro-environmental indicators to be integrated within a common administrative framework. The interpretation is therefore meso-scale and comparative, not household-level or site-specific. This scale limitation is important because the aggregation of environmental, demographic, and flood information to administrative boundaries may influence statistical relationships and spatial patterns, a well-known concern in spatial analysis described as the modifiable areal unit problem [20].

Jakarta provides a demanding case for this diagnostic framework because flooding in the city is shaped by interacting inland and coastal processes rather than by a single hazard mechanism. The metropolitan area lies on a low-lying coastal plain along the northwestern coast of Java and experiences flood-generating influences from intense rainfall, river connectivity, coastal water-level effects, land subsidence, dense urban development, and extensive land-surface modification. Process-based modelling for Jakarta has shown that elevated coastal water levels can restrict river drainage and

intensify flooding around river outlets, while continued subsidence and sea-level rise increase future coastal-flood exposure [5]. Broader studies of Asian megadeltas similarly emphasize that coastal flooding is shaped by interacting climatic, hydrological, geomorphic, and human-modification processes [6]. Recent InSAR evidence also confirms continuing land subsidence across Jakarta, reinforcing the need to represent subsidence-adjusted terrain conditions in flood assessment [21]. The location of Jakarta, the 261 *kelurahan* analytical units, and the principal spatial context used in this study are shown in Figure 1.

The empirical design used selected major flood observations during 2020-2024 to construct a multiyear observed burden proxy for each *kelurahan*. Rather than treating these observations as complete flood climatology, the study used them as a temporally consistent set of remotely sensed flood-event indicators. Hydro-environmental forcing was represented through climatic, topographic, hydrological, coastal, and land-surface variables, whereas the observed burden proxy was derived from the spatial coincidence between Sentinel-1 flood observations and gridded population exposure. This structure follows recent flood-exposure research showing that flood footprints become more meaningful for impact-oriented analysis when combined with spatial population data instead of interpreted only as inundated area [7], [8], [9].

All spatial datasets were harmonized to the *kelurahan* framework using a common boundary layer, consistent projection, and zonal processing. Raster variables with different native resolutions were summarized to each *kelurahan* according to their analytical role, including precipitation, elevation, slope, land subsidence, river proximity, coastline proximity, built-up intensity, impervious land cover, Sentinel-1 flood extent, and WorldPop population. Table 1 summarizes the datasets, temporal representation, analytical role, and principal uncertainty associated with each component. Detailed information on data sources, derived variables, transformations, analytical use, and major uncertainties is provided in Supplementary Table S1.

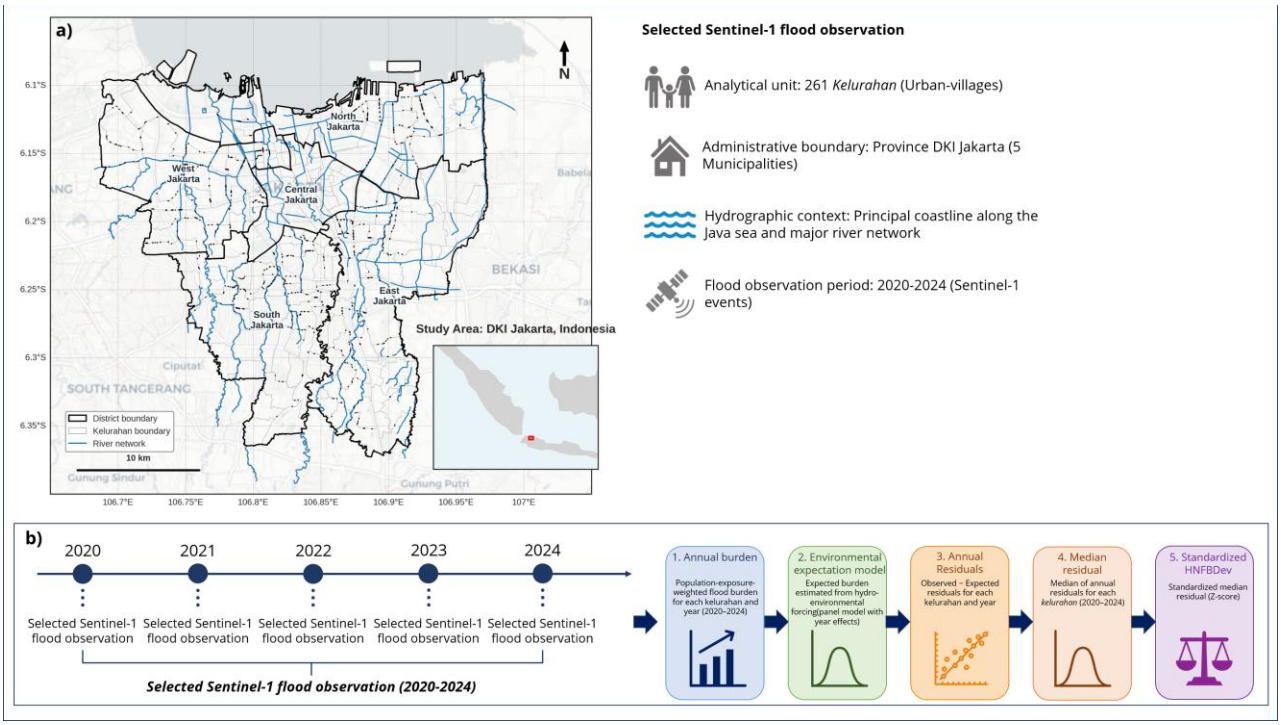


Fig. 1 Study area and observational framework. (a) Administrative boundaries of DKI Jakarta, Indonesia, showing the 261 *kelurahan* used as the spatial analysis units together with the major river network and surrounding geographic context. (b) Overview of the HNFBDev analytical workflow, where annual population-exposure-weighted observed burden is compared with the environmentally expected burden estimated from hydro-environmental forcing, followed by annual residual estimation, temporal median residual aggregation, and standardization to derive the Hazard-Normalized Flood Burden Deviation (HNFBDev).

Table 1 Data sources, temporal representation, analytical role, and principal uncertainty.

Component	Dataset or source	Native resolution	Temporal representation	Analytical role in HNFBDev	Principal uncertainty or limitation
Analytical boundary	Jakarta *kelurahan* administrative boundary	Vector	Static	Defines the 261 analytical units used for spatial harmonization, zonal aggregation, expectation modelling, and spatial diagnostics	Boundary aggregation may influence statistical relationships and spatial patterns through the modifiable areal unit problem
Coastline reference	Jakarta RBI coastline or equivalent	Vector	Static	Supports coastline proximity and	Shoreline representation may not

	national geospatial coastline layer			coastal-forcing construction	capture small engineered structures, reclamation, or short-term coastal modification
Precipitation forcing	CHIRPS daily precipitation	~0.05 degrees	Daily observations during 2020-2024, summarized as maximum daily precipitation during the study period	Represents atmospheric rainfall forcing within the inland and compound flood-generating baseline	Coarse spatial resolution relative to *kelurahan* scale; should be interpreted as study-period maximum rainfall forcing, not formal climatological Rx1day
Terrain elevation	Indonesian National Digital Elevation Model, DEMNAS	~8 m	Static terrain surface, adjusted for subsidence in the analytical workflow	Provides elevation and slope indicators affecting runoff accumulation, low-lying exposure, and coastal drainage gradients	DEM acquisition year and vertical accuracy may differ from 2020-2024 terrain conditions
Land subsidence	InSAR-derived Jakarta subsidence information	Raster or gridded surface	Cumulative displacement converted to annualized subsidence rate and extrapolated to the analytical period	Adjusts DEM-derived elevation to better represent effective terrain conditions during 2020-2024	Assumes temporally stationary subsidence rates; should be interpreted as first-order elevation adjustment rather than geodetic prediction
Hydrological connectivity	JRC Global Surface Water occurrence dataset	~30 m	Static long-term surface-water occurrence representation	Identifies permanent surface water and supports distance-to-water or river-	May omit small drainage channels, engineered canals, and temporary flow

				connectivity indicators	pathways relevant to local flooding
Built-up intensity	Sentinel-2 Harmonized Surface Reflectance	10 m	Study-period composite from 2020-2024	Derives built-up intensity using spectral contrast between built-up and vegetated surfaces	Cloud filtering, spectral mixing, and dense urban morphology may affect built-up signal
Surface impermeability	ESA WorldCover land-cover product	10 m	Static land-cover baseline	Provides impervious or permanently modified land-surface proxy influencing infiltration suppression and runoff generation	Land-cover classes simplify heterogeneous urban surfaces and may misclassify mixed built-up, vegetated, or coastal-modified areas
Flood observation	Sentinel-1 Ground Range Detected SAR imagery	~10 m	Selected major flood observations during 2020-2024	Provides remotely sensed flood extent used to construct annual observed burden proxy and multiyear observed burden proxy	Urban SAR flood mapping is affected by layover, radar shadow, double-bounce effects, threshold sensitivity, and incomplete flood-event representation
Population exposure	WorldPop gridded population estimates	~100 m	2020-2024 exposure representation based on available WorldPop surfaces and final harmonization strategy	Provides population exposure used to estimate population-exposure-weighted observed flood-burden proxy from the spatial coincidence of flood extent and population	Residential population does not represent daytime mobility, temporary displacement, or dynamic exposure during flood events

2.2 Hydro-environmental forcing and population-exposure-weighted burden proxy

Hydro-environmental forcing was constructed to represent the spatial conditions under which flood burden was expected to occur, before evaluating whether observed burden was unusually high or low. The forcing baseline was not intended to reproduce full hydraulic dynamics or to represent engineered flood-management performance. Instead, it summarized climatic, topographic, hydrological, coastal, and land-surface conditions that plausibly shape flood generation across Jakarta. This distinction is particularly relevant because the resulting HNFBDev values are interpreted as observed-expected burden deviations, not as direct measures of infrastructure performance, governance quality, adaptation success, or resilience. The analytical unit of this study was the *kelurahan* (n = 261). Observed burden was estimated separately for each annual flood event during 2020 –2024 and used as annual observations in the environmental expectation model. The model outputs were subsequently aggregated into a single HNFBDev value for each *kelurahan*. The analytical logic linking the forcing baseline, observed burden, expected burden, and HNFBDev interpretation boundary is summarized in Figure 2.

Two process domains were represented. The inland component represented rainfall-driven and terrain-mediated flood-generating conditions, including study-period maximum daily precipitation, subsidence-adjusted elevation, slope, proximity to permanent surface water, built-up intensity, and impervious land cover. The coastal component represented low-lying and coastal-connectivity conditions, including subsidence-adjusted elevation, coastline proximity, river and estuarine connectivity, study-period maximum daily precipitation, built-up intensity, slope, and impervious land cover. This dual structure follows the compound-flood literature, which recognizes that urban flooding in coastal cities results from interacting pluvial, fluvial, coastal, antecedent, and land-surface drivers rather than a single hazard source [1], [2], [3], [4]. It is also consistent with Jakarta-specific evidence showing that coastal water-level dynamics, river drainage obstruction, sea-level rise, and land subsidence jointly shape flood hazard in the northern part of the city [5], [6], [21].

Each indicator was transformed to a common 0–1 scale using percentile-based normalization and directional adjustment so that higher values consistently represented stronger flood-generating conditions. Literature-informed weights were then applied separately to the inland and coastal components, while equal weighting was retained for sensitivity analysis. For each component k, the normalized indicators X_{ij}were combined as:

$$H_{ki} = \sum_{j} w_{kj} X_{ij}$$

where H_{ki} is the inland or coastal forcing score for *kelurahan* i, w_{kj} is the component-specific weight assigned to indicator j, and X_{ij} is the normalized indicator value. The inland and coastal scores were then integrated using a fuzzy algebraic sum:

$$H_i = H_{i,inland} + H_{i,coastal} - \left(H_{i,inland} H_{i,coastal}\right)$$

This integration allows high inland or coastal forcing to contribute to the compound score while preventing simple double counting when both components are high. Indicator weights, forcing-component summary statistics, observed-burden proxy equations, and annual mapped flood extent are reported in Supplementary Table S2.

Flood burden was constructed from the spatial coincidence between remotely observed flood extent and gridded population exposure. Sentinel-1 Ground Range Detected imagery was used because synthetic aperture radar can observe inundation under cloud cover and is therefore well suited for event-based flood mapping in tropical urban environments. However, urban SAR flood detection remains affected by layover, radar shadow, double-bounce scattering, threshold sensitivity, and the masking of water surfaces in densely built-up areas; these limitations are particularly relevant for Jakarta's compact urban morphology [22], [23]. For this reason, the analysis distinguished between a stricter core flood mask and a more inclusive extended flood mask. The extended mask was used for the primary burden estimation, while the core mask was retained for sensitivity analysis. Event windows, orbit information, flood-mask thresholds, and filtering parameters are summarized in Supplementary Table S3.

For each selected flood event during 2020–2024, flood extent was derived using pre-event, event, and post-event Sentinel-1 observations, followed by permanent-water masking, terrain filtering, urban and non-urban thresholding, and connected-pixel filtering. The resulting flood masks were then intersected with gridded population data to estimate the event-specific exposed population within each kelurahan. This follows recent exposure studies showing that flood footprints become more informative when combined directly with high-resolution population surfaces rather than being interpreted solely as flooded area [7], [8], [9]. Event-specific observed burden was defined as:

$$E_{it} = \sum_{p \in F_{it}} Pop_{pit}$$

where E_{it} is the population-exposure-weighted observed flood-burden proxy in *kelurahan* i during event year t, F_{it} is the set of flooded pixels, and Pop_{pit} is the population assigned to pixel p. The resulting annual burden estimates were subsequently incorporated into the environmental expectation model described in Section 2.3 to derive the Hazard-normalized Flood Burden Deviation (HNFBDev). The observed burden represents a population-exposure-weighted flood-burden proxy rather than direct economic loss, flood depth, social vulnerability, or comprehensive disaster impact.

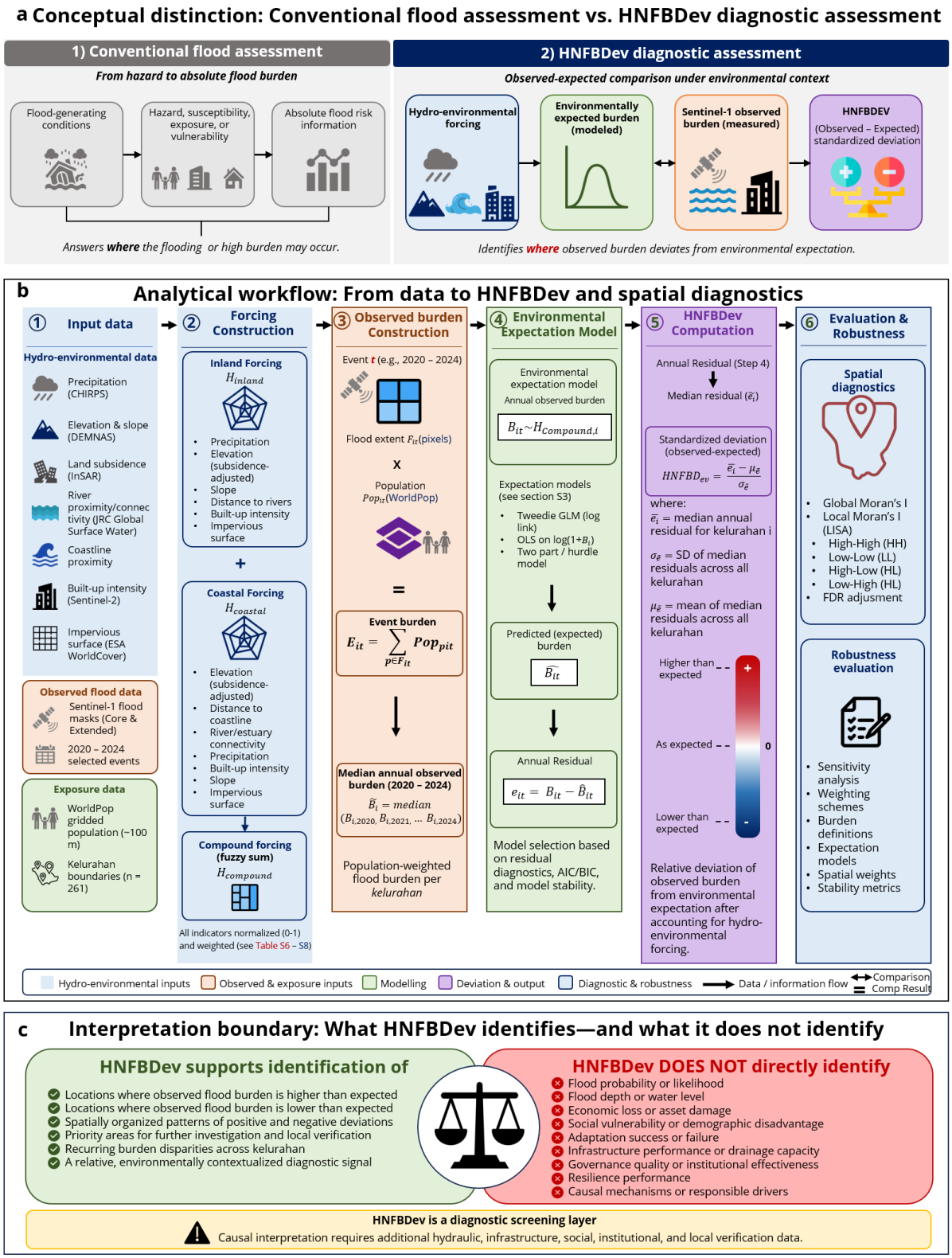


Fig. 2 Integrated conceptual and analytical framework for HNFBDev.

Figure 2 distinguishes conventional flood assessment from the HNFBDev observed-expected diagnostic approach; links hydro-environmental forcing, Sentinel-1 flood observations, gridded population exposure, environmental expectation modelling, HNFBDev computation, spatial diagnostics, and robustness testing; and clarifies that HNFBDev identifies relative flood-burden divergence but does not directly measure flood depth, social vulnerability, adaptation effectiveness, resilience, governance quality, infrastructure performance, or causal mechanisms.

2.3 Environmental expectation, HNFBDev, and diagnostic evaluation

Environmentally expected flood burden was estimated to determine the level of burden that would be anticipated under the represented hydro-environmental forcing conditions. The purpose of this model was not to predict flood impacts exhaustively, but to construct a defensible reference expectation against which observed burden could be compared. This follows the observed-expected logic used in reference-condition assessment, where the interpretation of an observed outcome depends on the environmental context under which that outcome occurs [16], [17], [18]. In the present study, the expected burden represents the modelled burden associated with the hydro-environmental baseline, while the remaining deviation represents the portion of observed burden not explained by that baseline.

Because annual flood-burden observations were non-negative, right-skewed, and occasionally contained zero or near-zero values, alternative model specifications were evaluated rather than relying on a single transformed linear model. Three candidate expectation models were considered: a generalized linear model with a Tweedie distribution and log link, an ordinary least-squares model using log-transformed annual observed burden, and a two-part (hurdle) specification separating the occurrence of non-zero burden from the magnitude of positive burden. This comparison reduced dependence on a single distributional assumption and addressed known limitations of log-transformed models under heteroskedasticity and non-normal error structures [24], [25]. The Tweedie specification was included because it can accommodate exact zeros and positive continuous outcomes within a unified generalized linear modelling framework [26].

The final environmental expectation model was selected through an iterative model development process that evaluated overall model adequacy, residual behaviour, information criteria, interpretability, and the stability of the resulting HNFBDev rankings. Because no single performance metric fully captures model suitability for this application, the selected specification reflects the best overall balance across these complementary evaluation criteria. As the objective of this study is the development of the HNFBDev diagnostic framework rather than comparative model assessment, only the final model specification is presented. Expected annual flood burden for kelurahan i in year t was denoted as $\hat{B}_{it}$, and the annual model residual was calculated as:

$$e_{it} = B_{it} - \hat{B}_{it}$$

Annual residuals were subsequently aggregated by taking the median residual across the 2020–2024 observation period for each kelurahan:

$$\tilde{e}_i = median(e_{i,2020}, \ldots e_{i,2024})$$

The Hazard-Normalized Flood Burden Deviation (HNFBDev) was then calculated by standardizing the median residuals:

$$HNFBDev_i = \frac{\bar{e}_i - \mu_{\bar{e}}}{\sigma_{\bar{e}}}$$

where $\bar{e}_i$ is the median annual residual for kelurahan *i*, $\mu_{\bar{e}}$ is the mean of the median residuals across all kelurahan, and $\sigma_{\bar{e}}$is the standard deviation of the median residuals across all kelurahan. Positive HNFBDev values indicate observed burden above environmental expectation, negative values indicate burden below environmental expectation, and values near zero indicate that the observed burden is broadly consistent with the environmental expectation. These values were interpreted as relative spatial deviations rather than direct indicators of hazard probability, flood depth, vulnerability, infrastructure performance, governance quality, or adaptation effectiveness. The environmental expectation model, residual diagnostics, and model-scale checks are summarized in Supplementary Table S3.

Spatial diagnostics were used to determine whether HNFBDev values were geographically organized rather than randomly distributed across Jakarta. Global Moran's I was first calculated to test whether positive and negative deviations exhibited overall spatial autocorrelation. Local Moran's I was then used to identify localized clusters and spatial outliers, including High-High, Low-Low, High-Low, and Low-High configurations [27]. Because local spatial statistics involve repeated tests across many spatial units, false-discovery-rate adjustment was considered to reduce the likelihood of overstating local cluster significance [28]. The primary spatial-weight matrix used the k-nearest-neighbour specification available in the current spatial output, while contiguity-based alternatives can be retained for sensitivity testing if the analysis is rerun. These choices were documented because spatial autocorrelation statistics can vary with neighbourhood definition, weight standardization, and software implementation [29].

The spatial analysis was interpreted diagnostically. A significant Global Moran's I indicates that unexplained deviations are spatially structured, while Local Moran classes identify where similar or contrasting deviations occur among neighbouring units. However, residual clustering does not by itself establish the causes of those deviations. Spatially organized residuals may reflect omitted spatial processes, unmeasured infrastructure or exposure conditions, model misspecification, measurement uncertainty, or genuine spatial disparities in realized burden. This interpretation follows broader cautions that residual spatial autocorrelation can indicate unrepresented spatial structure rather than automatically validating a model or mechanism [30].

Robustness was evaluated across analytical dimensions. First, the hydro-environmental forcing surface was recalculated using literature-informed weights and equal weights. Second, observed burden was compared under different Sentinel-1 flood-mask assumptions where outputs were available. Third, HNFBDev was compared across alternative expectation-model specifications and burden definitions where final outputs were available. Fourth, Global Moran's I, Local Moran classifications, and cluster membership can be recalculated under alternative spatial-weight matrices when the final sensitivity analysis is completed. Stability was summarized using Pearson correlation, Spearman rank correlation, RMSE, and cluster-class agreement where available. Spatial-diagnostic outputs, Local Moran's I cluster counts, highest positive HNFBDev locations, and AHP-equal-weight robustness statistics are provided in Supplementary Table S4.

3. Results

3.1 Hydro-environmental forcing and population-exposure-weighted burden proxy

Hydro-environmental forcing varied substantially across Jakarta, confirming that the environmental conditions under which flood burden occurs are not spatially uniform across the 261 *kelurahan*. The inland forcing component showed moderate spatial variation, with a mean of 0.711, standard deviation of 0.085, median of 0.676, and range from 0.420 to 0.894 (Fig. 3a). This distribution indicates that rainfall-related, terrain-mediated, hydrological, and land-surface flood-generating conditions are present across much of Jakarta, although their relative intensity differs among *kelurahan*. By contrast, the coastal forcing component was more spatially selective, with a mean of 0.095, standard deviation of 0.189, median of 0.000, and range from 0.000 to 0.798 (Fig. 3b). This strongly skewed distribution reflects the concentration of coastal and estuarine influences in the northern part of the city rather than across the entire metropolitan area.

The compound forcing surface integrated the inland and coastal components into a single hydro-environmental reference condition for expectation modelling. The compound literature-informed forcing score had a mean of 0.733, standard deviation of 0.102, median of 0.725, and range from 0.420 to 0.945 (Fig. 3c). The equal-weight compound specification produced a similar distribution, with a mean of 0.758, standard deviation of 0.101, median of 0.757, and range from 0.472 to 0.959. This similarity indicates that the broad forcing pattern was not driven solely by the literature-informed weighting scheme. The compound map therefore provides the environmental baseline for estimating expected flood burden, while the equal-weight version is retained for robustness assessment.

The annual flood record derived from five selected Sentinel-1 flood events showed clear interannual variation. Mapped flood extent increased from 43.76 km² in 2020 to 45.63 km² in 2021 and 46.42 km² in 2022, before declining to 34.54 km² in 2023 and remaining relatively stable at 34.69 km² in 2024. The mean annual mapped flood extent across the selected observations was 41.01 km2. These values should be interpreted as event-based remote-sensing observations used to construct flood burden, not as a continuous

flood climatology or a hydraulic measure of flood depth. To derive the observed burden into a burden-oriented outcome, annual flood occurrence was combined with population exposure at the *kelurahan* level. The resulting observed burden increased where inundation coincided with higher population concentration, while sparsely populated or weakly inundated areas contributed less to the observed burden (Fig. 3d-f).

The spatial pattern of observed burden did not directly mirror the hydro-environmental forcing surface. Areas with stronger compound forcing identified environmental settings where higher burden would be expected, but observed burden also reflected the uneven location of exposed population and the event-specific distribution of mapped inundation. Several *kelurahan* with broadly similar hydro-environmental forcing therefore exhibited different realized burden levels, while some locations with moderate forcing still displayed elevated exposure-weighted burden. This mismatch between forcing and observed burden forms the basis for the observed-expected analysis developed in the next subsection.

Taken together, Figure 3 shows that Jakarta's flood-burden geography cannot be explained from environmental forcing, mapped flood extent, or population exposure alone. The hydro-environmental maps identify where flood-generating conditions are stronger, whereas the observed-burden map identifies where selected flood observations intersected with exposed population. The next analytical step is therefore to estimate whether each *kelurahan*'s observed burden is higher or lower than expected under its represented hydro-environmental setting.

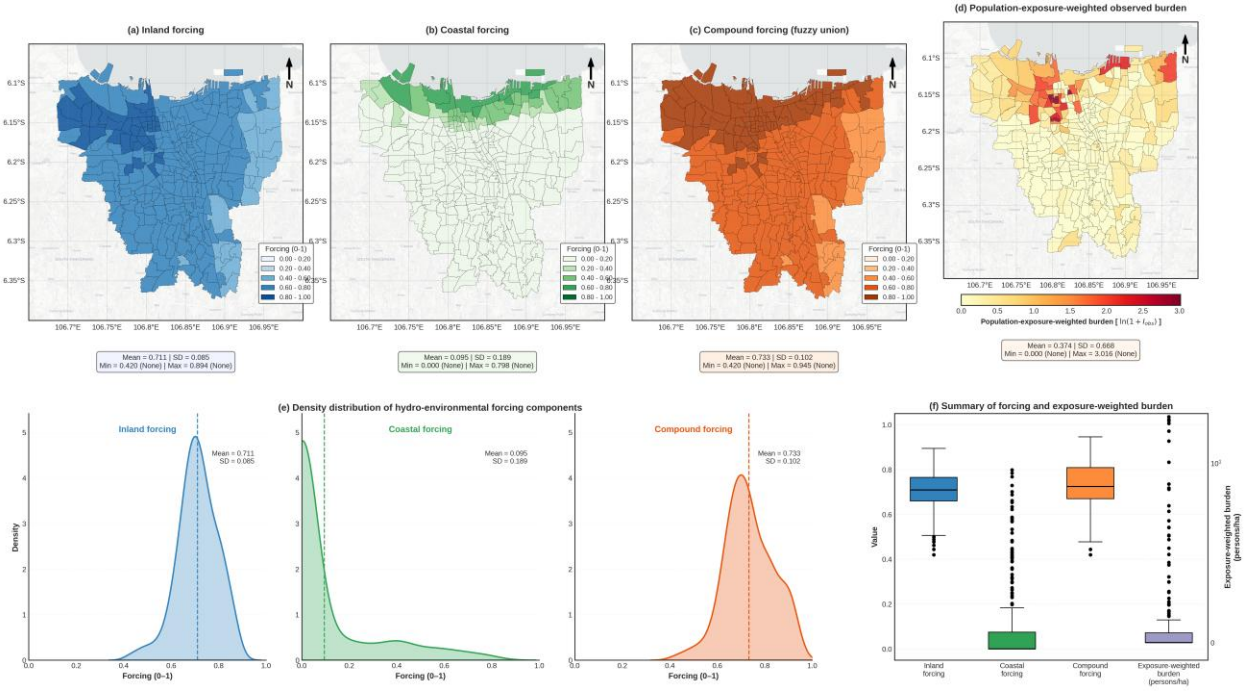


Fig. 3 Hydro-environmental forcing and observed flood burden. (a) Inland hydro-environmental forcing. (b) Coastal hydro-environmental forcing. (c) Compound hydro-environmental forcing derived from the integration of inland and coastal components. (d)

Population-exposure-weighted observed burden aggregated at the kelurahan level. (e) Probability density distributions of the hydro-environmental forcing components. (f) Comparative distribution of hydro-environmental forcing and observed burden across Jakarta.All maps are displayed for 261 kelurahan.

3.2 Environmentally expected burden and spatial disparities

The environmental expectation model showed a strong positive relationship between compound hydro-environmental forcing and population-exposure-weighted burden proxy. The forcing coefficient was 3.172, with a standard error of 0.162, t-statistic of 19.565, and p-value below 0.001. The model explained 22.8% of the variation in population-exposure-weighted burden proxy, with an adjusted R^2 of 0.225 and an overall F-statistic of 76.93 based on 1,305 *kelurahan*-year observations. These result indicates that stronger represented flood-generating conditions were associated with higher expected burden, but it also shows that most variation in realized burden remained outside the hydro-environmental baseline. In other words, the hydro-environmental forcing surface provided a statistically meaningful reference for expectation modelling, but it did not fully determine where flood burden was realized (Fig. 4a-b).

The expected-burden surface was smoother than the observed-burden surface because it was estimated from the spatial organization of compound hydro-environmental forcing. This distinction is analytically useful. The expected surface identifies the burden level that would be anticipated underrepresented environmental conditions, while the observed surface captures where mapped inundation intersected with population exposure during the selected flood observations. The difference between the two surfaces produced HNFBDev, which identifies *kelurahan* where observed burden was higher or lower than environmental expectation. Positive values therefore indicate higher-than-expected burden, negative values indicate lower-than-environmentally expected burden, and values near zero indicate broad agreement between observed burden and the environmental expectation (Fig. 4c-d).

The standardized HNFBDev distribution was asymmetric around the expectation baseline. Most *kelurahan* clustered within approximately one standard deviation of zero, indicating that observed burden generally remained close to the environmentally expected level. However, the positive tail extended beyond three standard deviations, while negative deviations were less extreme. The HNFBDev summary statistics support this pattern: standardized HNFBDev values derived using the literature-informed weighting scheme had a mean near zero, standard deviation of approximately one, median of -0.246, minimum of -1.772, and maximum of 3.83. This indicates that unusually high positive deviations were more pronounced than unusually low negative deviations. The largest positive deviations occurred in Tangki, Kota Bambu Utara, Jembatan Besi, Duri Selatan, and Duri Utara, with HNFBDev values ranging from 3.56 to 3.83. These locations represent persistent higher-than-expected burden under the represented hydro-environmental baseline, not direct evidence of adaptation failure, infrastructure underperformance, or governance weakness.

The spatial distribution of HNFBDev revealed substantial intra-urban heterogeneity after hydro-environmental normalization. Positive deviations were concentrated mainly in northern and central Jakarta, while negative deviations appeared more frequently across parts of southern and western Jakarta. These patterns differed from both the compound forcing surface and the expected-burden surface, indicating that *kelurahan* with comparable hydro-environmental settings could still experience different realized burden levels. The resulting map therefore provides a complementary diagnostic layer that complements the forcing and observed-burden maps shown in Figure 3.

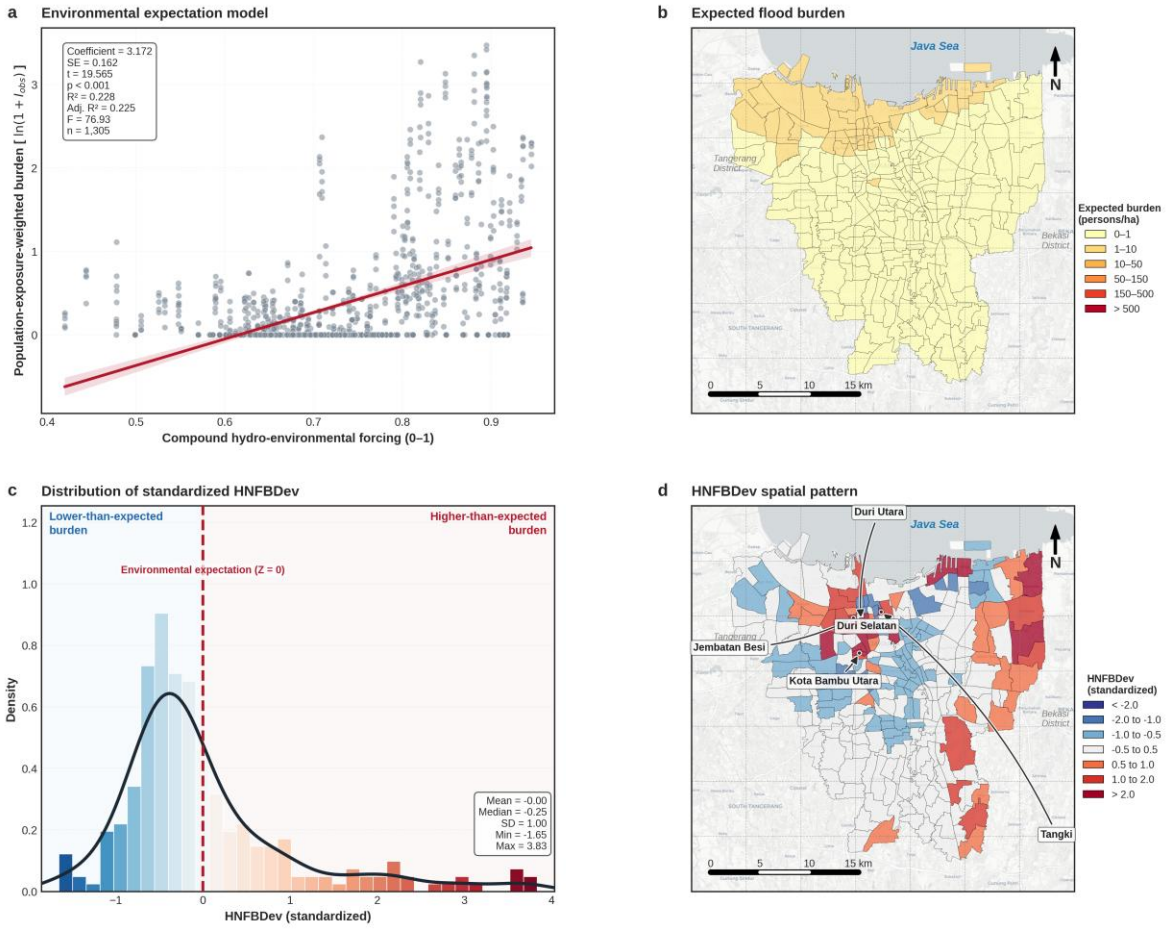


Fig. 4 Environmental expectation model and spatial deviations from environmentally expected flood burden. (a) Relationship between compound hydro-environmental forcing and the population-exposure-weighted observed burden used to estimate the environmental expectation model. (b) Spatial distribution of the environmentally expected burden proxy. (c) Distribution of standardized Hazard-Normalized Flood Burden Deviation (HNFBDev); the dashed vertical line denotes the environmental expectation (Z = 0), with values below and above zero representing lower-than-expected and higher-than-expected burden, respectively. (d) Spatial distribution of HNFBDev across Jakarta, highlighting localized deviations between observed and environmentally expected flood burden.

3.3 Spatial organization and robustness of HNFBDev

The HNFBDev surface exhibited statistically significant spatial organization rather than being randomly distributed patterns of observed-expected deviations. Global Moran's I was 0.355 with a permutation significance level of p = 0.001, indicating moderate positive spatial autocorrelation among neighboring *kelurahan* (Fig. 5a). *Kelurahan* with positive HNFBDev values therefore tended to be located near other *kelurahan* with similarly positive deviations, while negative values were also geographically clustered. These results support the interpretation that higher- and lower-than-expected flood burden patterns are spatially structured after accounting for the represented hydro-environmental baseline.

Local Moran's I further identified distinct clusters and spatial outliers of HNFBDev. Most *kelurahan* were not statistically significant local clusters, with 174 units, or 66.67% of the study area, classified as not significant. Among significant local associations, Low-Low clusters were the most frequent, covering 44 *kelurahan*, or 16.86%, followed by High-High clusters covering 29 *kelurahan*, or 11.11%. Spatial outliers were less common: 8 *kelurahan*, or 3.07%, were classified as Low-High, and 6 *kelurahan*, or 2.30%, were classified as High-Low (Fig. 5b). The predominance of High-High and Low-Low clusters over spatial outliers indicates that the observed-expected deviations were characterized mainly by coherent neighborhood-scale clustering rather than by isolated anomalous units.

The interpretation of these spatial clusters remains diagnostic. High-High clusters identify groups of neighboring *kelurahan* where population-exposure-weighted burden proxy was consistently higher than expected under the represented hydro-environmental setting. Low-Low clusters identify neighboring *kelurahan* where observed burden was lower than expected. High-Low and Low-High outliers mark transition areas where local HNFBDev values differed from adjacent units. These cluster classes should not be interpreted as direct evidence of adaptation success, adaptation failure, infrastructure performance, governance quality, or causal mechanisms. Instead, they indicate where further hydraulic, infrastructure, exposure, social, institutional, and local verification data are needed to explain why observed burden diverged from environmental expectation.

The robustness assessment showed that HNFBDev was highly stable under alternative hydro-environmental weighting assumptions. Comparing the literature-informed weighted forcing with the equal-weight specification produced a Pearson correlation of r = 0.990, a Spearman rank correlation of rho = 0.970, and an RMSE of 0.146 (Fig. 5c). This high agreement indicates that the main HNFBDev ranking and spatial pattern were not driven primarily by the selected weighting scheme. Instead, the diagnostic pattern was largely preserved when the same indicators were recombined using equal weights. Residual diagnostics indicated statistically significant heteroskedasticity and non-normality, with residual magnitude increasing under higher expected-burden conditions. HNFBDev should therefore be interpreted as a relative spatial diagnostic rather than a variance-independent performance metric.

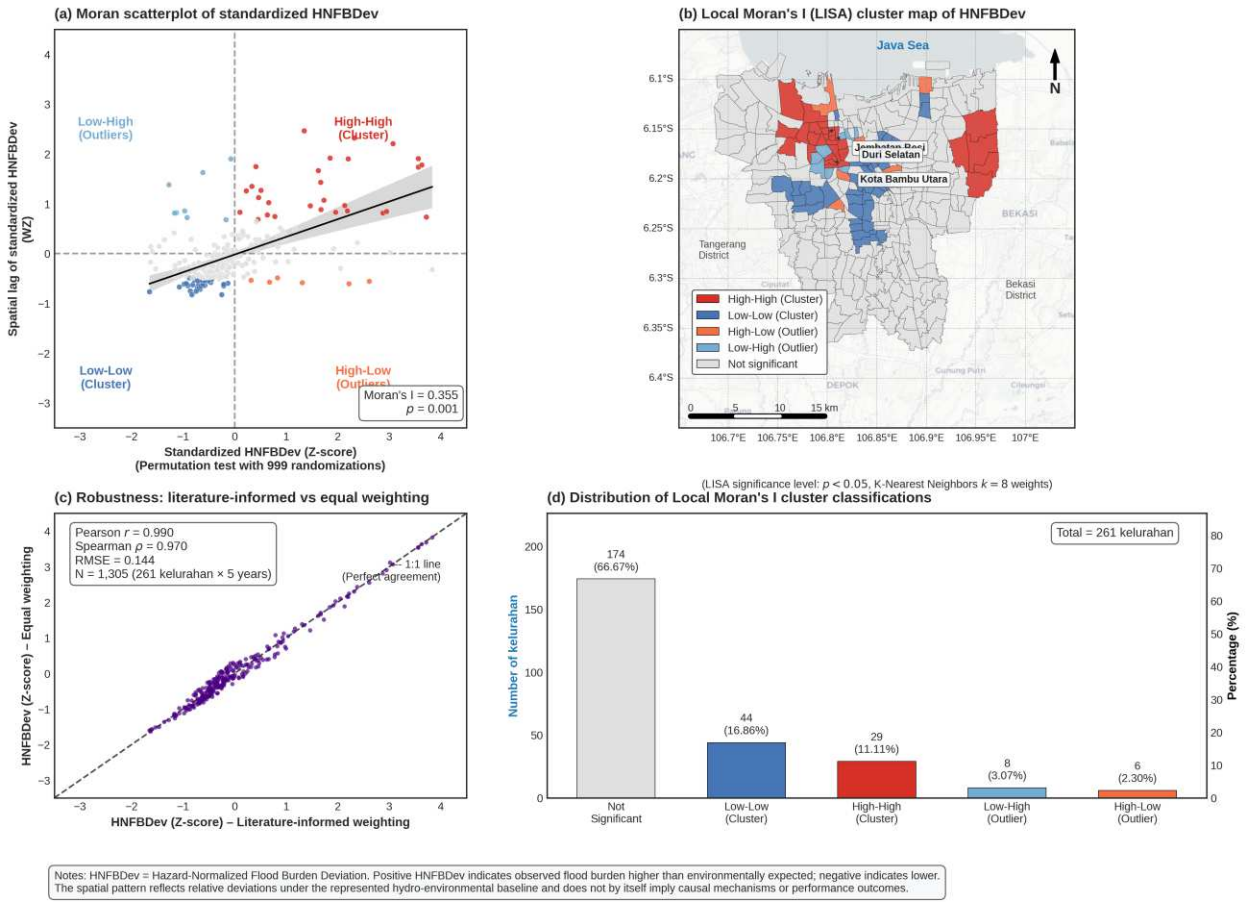


Fig. 5 Spatial organization and robustness of HNFBDev across Jakarta. (a) Local Indicators of Spatial Association (LISA) identifying statistically significant spatial clusters of HNFBDev. (b) Global spatial autocorrelation of HNFBDev evaluated using Moran's I. (c) Robustness assessment comparing literature-informed weighting and equal-weight hazard formulations, demonstrating the consistency of HNFBDev spatial patterns under alternative hazard aggregation schemes.

4. Discussion

4.1 Contribution beyond conventional flood assessment

The results show that hydro-environmental forcing, population-exposure-weighted burden proxy, and observed-expected deviation describe different aspects of Jakarta's urban flood geography. The compound forcing surface identified where represented flood-generating conditions were stronger, while the observed-burden surface showed where selected Sentinel-1 flood observations intersected with exposed population. The expectation model then provided an environmental reference against which observed burden could be compared. This distinction is central because the expectation model explained 22.8% of the variation in the population-exposure-weighted burden proxy variation, leaving most spatial variation outside the represented hydro-environmental baseline. The remaining variation should not be dismissed as statistical noise; it defines

the diagnostic space in which HNFBDev identifies *kelurahan* where burden is higher or lower than expected under comparable represented conditions.

This contribution complement, rather than replaces, established approaches in urban flood assessment. Hydrodynamic modelling, flood-susceptibility mapping, and compound-hazard analysis remain essential for identifying where flood-generating processes may occur, particularly in cities where pluvial, fluvial, coastal, drainage, and antecedent conditions interact [1], [2], [3], [4]. Satellite-based flood mapping and global exposure studies have further improved the ability to estimate where inundation intersects with population and assets, moving flood assessment beyond hazard footprints alone [7], [8], [9]. Yet these approaches usually describe absolute hazard, absolute exposure, or absolute burden. HNFBDev adds a complementary diagnostic layer by asking whether realized burden is unusually high or low relative to the environmental setting in which it occurs.

The need for this relative diagnostic is supported by flood-impact and vulnerability literature. Flood consequences are not determined by physical inundation alone; they depend on the interaction of hazard intensity, exposed population, asset distribution, protection systems, preparedness, institutional response, and social vulnerability [10], [11], [13]. Recent work also shows that flood exposure and flood risk can be socially and spatially uneven within urban areas, including at neighborhood scale [12], [15]. HNFBDev contributes to this literature by separating two questions that are often conflated: where flood-generating conditions are strong, and where realized burden is higher or lower than expected under those conditions.

Conceptually, this approach draws from observed-expected and reference-condition reasoning in ecological and environmental assessment, where observed states are interpreted against conditions expected under comparable environmental settings [16], [17], [18]. This logic is useful for flood-burden assessment because Jakarta's *kelurahan* differs substantially in terrain, hydrological connectivity, coastal influence, land-surface modification, and exposure. A high observed burden in a highly flood-prone *kelurahan* has a different diagnostic interpretation from the same burden in a more moderate environmental setting. At the same time, observed-expected residuals require statistical caution because residual variance can depend on the expected value and can be affected by model specification, spatial dependence, and measurement uncertainty [19], [30]. For this reason, HNFBDev is best understood as a comparative diagnostic layer, not as a direct measure of adaptation effectiveness, resilience, infrastructure performance, or governance quality.

4.2 Interpreting spatially organized burden disparities

The clustered HNFBDev patterns suggest that observed-expected flood-burden disparities are not isolated anomalies. High-High clusters identify neighboring *kelurahan* where observed burden was higher than expected under the represented hydro-environmental setting, while Low-Low clusters identify neighboring *kelurahan* where observed burden was lower than expected. This spatial organization matters because

flood outcomes in Jakarta are shaped by connected drainage systems, river corridors, low-lying coastal terrain, backwater effects, land subsidence, urban form, and population concentration rather than solely by independent local conditions. Jakarta-specific modelling has shown that coastal water levels can obstruct drainage and intensify flooding near river outlets, while sea-level rise and subsidence increase future coastal exposure [5]. More broadly, Asian megadeltas face interacting pressures from climate change, subsidence, land-use change, and engineered modification of deltaic systems [6].

The interpretation of these clusters should remain diagnostic. A High-High cluster does not automatically indicate weak infrastructure, poor governance, or failed adaptation. It indicates that several neighboring *kelurahan* experienced higher observed burden than expected after accounting for represented hydro-environmental forcing. Possible explanations include drainage bottlenecks, local flood-control condition, flood-path connectivity, settlement morphology, exposure concentration, event-specific flood dynamics, or social vulnerability. It may also reflect measurement uncertainty in Sentinel-1 flood detection or unrepresented processes in the environmental expectation model. Similarly, a Low-Low cluster should not be treated as proof of resilience or successful adaptation. Lower-than-expected burden may reflect effective protection, lower exposed population, favorable local drainage, topographic advantages, incomplete flood detection, or model limitations.

This caution is consistent with compound-risk and disaster-impact literature. Compound flood outcomes can emerge from interacting drivers whose joint effects are not captured by a single forcing variable [1], [2], [3]. Risk-management studies further show that impacts may be reduced, displaced, or amplified depending on protection, preparedness, institutional capacity, and residual risk conditions [11], [31], [32]. In urban settings, these interactions can create spatial disparities in realized burden even when broad environmental conditions appear similar. HNFBDev is useful because it does not directly infer underlying mechanisms; instead, it identifies where such mechanisms warrant further investigation

The spatial-statistical results also require careful interpretation. Moran's I and Local Moran's I show that HNFBDev values are spatially organized, but they do not explain why clustering occurs [27]. Local clusters may indicate real spatial processes, but they may also arise from omitted variables, aggregation effects, neighborhood definitions, or residual spatial dependence [29], [30]. For Jakarta, the practical implication of these findings is that HNFBDev clusters should guide field verification and multi-source triangulation. High-High areas should be examined for drainage constraints, repeated flood pathways, settlement exposure, and infrastructure conditions. Low-Low areas should be examined to determine whether lower-than-expected burden reflects protection, lower exposure, favorable local hydrology, or data limitations. Figure 6 summarizes these interpretation pathways and illustrates how HNFBDev can be used as part of a cautious planning sequence.

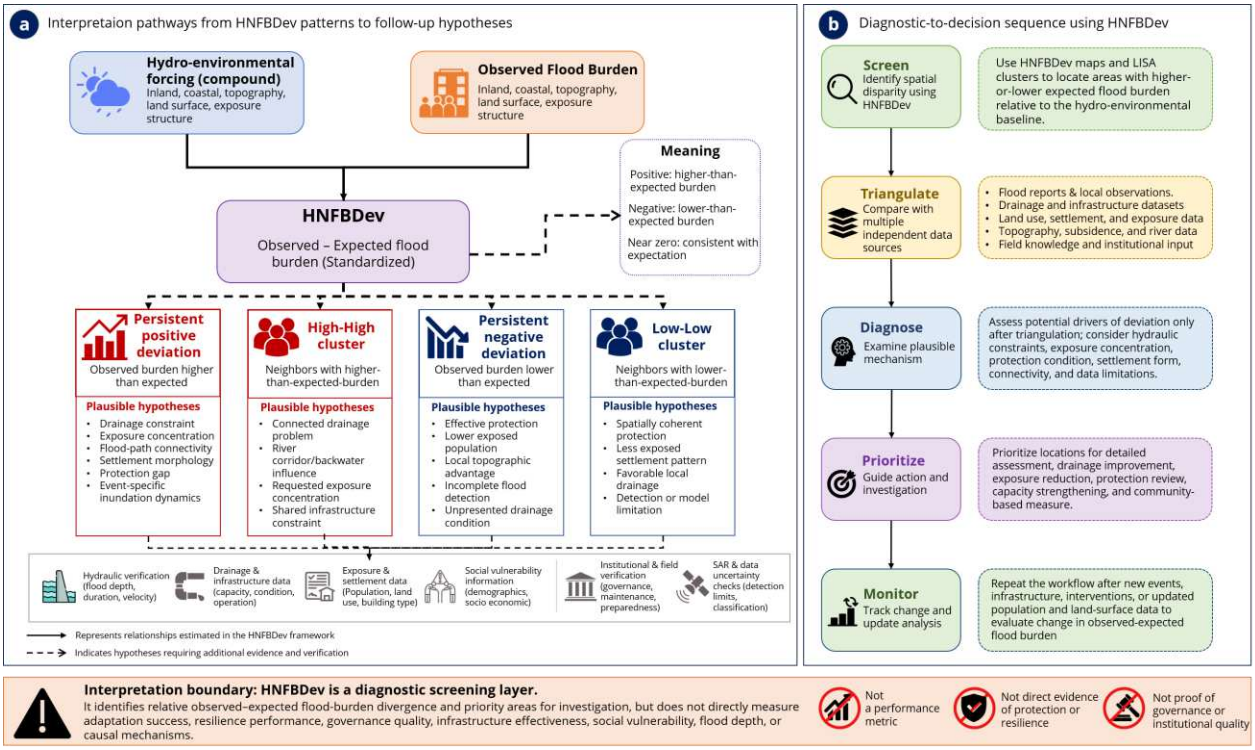


Fig. 6 Interpretation framework for Hazard-Normalized Flood Burden Deviation (HNFBDev). (a) Conceptual interpretation of HNFBDev as the deviation between observed and environmentally expected flood burden after accounting for hydro-environmental forcing. (b) Interpretation boundary illustrating that positive and negative HNFBDev values represent spatial departures from environmental expectation rather than direct measures of adaptation performance or causal mechanisms. (c) Framework for interpreting HNFBDev as a spatial diagnostic tool for identifying areas with systematically higher-than-expected or lower-than-expected flood burden and generating hypotheses for further investigation.

4.3 Planning applications, transferability, and limitations

HNFBDev is most useful as a screening and prioritization tool within a broader flood-risk assessment workflow. In Jakarta, the diagnostic identifies *kelurahan* where observed burden is higher or lower than expected under represented hydro-environmental conditions. This information can help planners decide where to examine drainage constraints, exposure concentration, flood-path connectivity, protection condition, settlement morphology, or local response capacity in more detail. It can also help avoid over-prioritizing locations solely because they have high absolute burden, when that burden may be consistent with strong environmental forcing. Conversely, moderate-forcing locations with higher-than-expected burden may deserve closer attention because they indicate realized burden that is disproportionate to the represented environmental baseline. This use is aligned with broader calls for geospatial monitoring systems that support urban climate resilience, situational awareness, and planning-oriented diagnostics [33], [34].

The framework is transferable to other cities, but only if the environmental baseline and burden metric are locally meaningful. Coastal megacities, deltaic settlements, riverine cities, inland basins, and rapidly urbanizing peri-urban areas differ in the relative importance of rainfall, drainage, river discharge, coastal water levels, subsidence, land cover, and exposure distribution [4], [6]. The HNFBDev framework is therefore more readily transferable than any specific indicator set or weighting scheme. In cities with strong hydrodynamic models, drainage-network data, infrastructure inventories, household exposure records, or verified flood-depth observations, HNFBDev could be integrated with those datasets to strengthen interpretation. In data-constrained settings, it can still provide an initial observed-expected screening layer, but planning decisions should be supported by local verification.

Several limitations should guide interpretation. First, the Sentinel-1 flood observations represent selected major events during 2020-2024, not a complete flood climatology. SAR-based flood mapping is valuable because it can observe inundation under cloud cover, but urban detection remains affected by layover, radar shadow, double-bounce scattering, threshold sensitivity, permanent-water masking, and the complex geometry of built environments [22], [23]. Second, the observed burden metric represents population-exposure-weighted flood burden, not flood depth, duration, direct economic loss, household damage, or social vulnerability. Flood-loss studies have consistently emphasized that consequences are difficult to infer from inundation extent alone because damage depends on depth, duration, assets, preparedness, and local vulnerability conditions [10], [13].

Statistical and spatial limitations also remain. The expectation model uses represented hydro-environmental forcing to estimate expected burden, but it does not directly include drainage capacity, pump operation, infrastructure condition, informal drainage modification, emergency response, or household-level behavior. Residual diagnostics suggest heteroskedasticity and non-normality, which is a known challenge when modelling skewed, non-negative outcomes using transformed linear models or residual-based diagnostics [24], [25], [26]. Spatial aggregation to *kelurahan* boundaries may also influence estimated relationships and cluster patterns, consistent with the modifiable areal unit problem [20]. These limitations do not invalidate the diagnostic, but they define its proper use: HNFBDev identifies where observed burden diverges from environmental expectation and where further investigation is most justified. Table 2 summarizes the interpretation, evidence needs, planning relevance, and conclusions to avoid for each major HNFBDev pattern.

Table 2 Interpretation, evidence needs, and planning relevance of HNFBDev patterns.

HNFBDev pattern	Defensible interpretation	Evidence required next	Appropriate planning use	Conclusion to avoid
Persistent higher-than-expected burden	Observed burden is higher than expected	Drainage condition, flood-depth or duration data,	Prioritize local investigation and diagnose possible	Do not infer adaptation failure, governance weakness, or

	under represented hydro-environmental conditions	local exposure, infrastructure operation, settlement morphology, field verification	burden-amplifying mechanisms	infrastructure underperformance directly
High-High cluster	Neighboring *kelurahan* show higher-than-expected burden	River-corridor assessment, drainage-network connectivity, shared infrastructure condition, repeated flood reports, exposure concentration	Identify neighborhood-scale priority zones for integrated flood-risk review	Do not assume a single shared cause without additional evidence
High-Low outlier	A high positive-deviation *kelurahan* is surrounded by lower-deviation neighbors	Local drainage blockage, land-use discontinuity, localized exposure, flood-mask uncertainty, boundary effects	Target site-specific verification and check local anomalies	Do not treat the surrounding neighborhood as equally burdened
Near-zero deviation	Observed burden is broadly consistent with environmental expectation	Model diagnostics, flood-observation reliability, exposure consistency	Use as reference condition for comparison and monitoring	Do not interpret as low risk or absence of flood concern
Persistent lower-than-expected burden	Observed burden is lower than expected under represented hydro-environmental conditions	Protection condition, topographic advantage, lower exposure, incomplete flood detection,	Examine whether lower burden reflects protection, lower exposure, or data limitations	Do not infer resilience or adaptation success directly

		local hydrology		
Low-Low cluster	Neighboring *kelurahan* show lower-than-expected burden	Shared protection systems, drainage performance, lower exposure patterns, SAR-detection checks, local verification	Identify potential learning areas after confirming mechanisms	Do not assume proven protection effectiveness without validation

5. Conclusions

Urban flood assessment often begins by asking where hazards, exposure, or vulnerability are greatest. This study advances a complementary question: where is flood burden higher or lower than would be expected after accounting for the hydro-environmental setting in which that burden occurs? By developing HNFBDev as an observed-expected diagnostic, the study shows that flood-burden disparities can be examined not only as absolute outcomes, but also as deviations from an environmental expectation. This distinction is particularly relevant for complex coastal and deltaic cities, where rainfall, drainage, river connectivity, coastal influence, subsidence, land-surface modification, and population exposure interact unevenly across urban space.

The Jakarta application demonstrates that environmentally contextualized flood-burden diagnosis can reveal patterns that are not visible from hazard, exposure, or observed inundation maps alone. Compound hydro-environmental forcing was associated with the population-exposure-weighted burden proxy, but it did not fully explain where burden was realized. The remaining observed-expected deviations were spatially organized and robust under alternative weighting assumptions, indicating that relative flood-burden disparities are not merely local anomalies or artefacts of one weighting scheme. These findings support the value of HNFBDev as a diagnostic layer for identifying places where flood outcomes deserve closer investigation.

The broader contribution is methodological and transferable. HNFBDev provides a way to satellite-derived flood observations, population exposure, environmental normalization, and spatial diagnostics into an unified framework for urban flood assessment. It can help cities move beyond ranking places only by absolute hazard or exposure, toward identifying where realized burden appears disproportionate to represented flood-generating conditions. This is especially relevant for rapidly urbanizing coastal and deltaic regions where detailed hydrodynamic, infrastructure, and social data are often incomplete.

The framework should be used with caution. HNFBDev does not directly measure flood depth, economic loss, social vulnerability, infrastructure effectiveness, governance quality, resilience, adaptation performance, or causal mechanisms. Its value lies in identifying where further investigation is warranted. Used in this way, HNFBDev can support a more diagnostic, evidence-oriented, and globally relevant approach to understanding uneven urban flood burden under changing climatic and urban conditions.

Acknowledgements
The authors acknowledge the providers of the open geospatial, satellite, population, precipitation, terrain, and land-cover datasets used in this study. The authors also acknowledge institutional and technical support that enabled the development of the analytical workflow. Specific project, institutional, and funding acknowledgements should be inserted after the author team and funding source are finalized.

Author contributions
Perdinan: Conceptualization, Methodology, Supervision, Writing, Review, and Editing
Rifky Husaini: Data curation, Formal analysis, Investigation, Visualization, Software, Writing – Original Draft.
Novindra: Supervision and inputs

Funding Statement
This research did not receive any specific funding support.

Data Availability Statement
The geospatial datasets used in this study are derived from publicly available remote-sensing, population, land-cover, precipitation, terrain, and surface-water sources, combined with administrative boundary and coastline data for Jakarta. Processed intermediate datasets, model outputs, and spatial diagnostic results can be made available by the corresponding author upon reasonable request, subject to data-use conditions and repository preparation. The Supplementary Information provides details on data sources, preprocessing steps, indicator construction, model specifications, and robustness procedures.

Code availability
The analytical workflow was implemented using Google Earth Engine and Python-based geospatial and statistical processing. Code used for flood-mask extraction, hydro-environmental forcing construction, observed-burden calculation, expectation modelling, spatial diagnostics, and robustness assessment can be made available by the corresponding author upon reasonable request after repository cleaning and documentation.

Declarations

Clinical trial number
Not applicable

Ethics approval and consent to participate
Not applicable

Consent for publication
Not applicable

Competing interests
Not applicable

References

[1] J. Zscheischler *et al.*, “Future climate risk from compound events,” Jun. 01, 2018, *Nature Publishing Group*. doi: 10.1038/s41558-018-0156-3.

[2] T. Wahl, S. Jain, J. Bender, S. D. Meyers, and M. E. Luther, “Increasing risk of compound flooding from storm surge and rainfall for major US cities,” *Nat. Clim. Chang.*, vol. 5, no. 12, pp. 1093–1097, Dec. 2015, doi: 10.1038/nclimate2736.

[3] A. Couasnon *et al.*, “Measuring compound flood potential from river discharge and storm surge extremes at the global scale,” *Natural Hazards and Earth System Sciences*, vol. 20, no. 2, pp. 489–504, Feb. 2020, doi: 10.5194/nhess-20-489-2020.

[4] J. Green *et al.*, “Review article: A comprehensive review of compound flooding literature with a focus on coastal and estuarine regions,” Feb. 20, 2025, *Copernicus Publications*. doi: 10.5194/nhess-25-747-2025.

[5] W. G. Bennett *et al.*, “Modelling compound flooding: a case study from Jakarta, Indonesia,” *Natural Hazards*, vol. 118, no. 1, pp. 277–305, Aug. 2023, doi: 10.1007/s11069-023-06001-1.

[6] M. Becker *et al.*, “Coastal Flooding in Asian Megadeltas: Recent Advances, Persistent Challenges, and Call for Actions Amidst Local and Global Changes,” Dec. 01, 2024, *John Wiley and Sons Inc*. doi: 10.1029/2024RG000846.

[7] B. Tellman *et al.*, “Satellite imaging reveals increased proportion of population exposed to floods,” *Nature*, vol. 596, no. 7870, pp. 80–86, 2021, doi: 10.1038/s41586-021-03695-w.

[8] A. Smith, P. D. Bates, O. Wing, C. Sampson, N. Quinn, and J. Neal, “New estimates of flood exposure in developing countries using high-resolution population data,” *Nat. Commun.*, vol. 10, no. 1, p. 1814, Apr. 2019, doi: 10.1038/s41467-019-09282-y.

[9] J. Rentschler, M. Salhab, and B. A. Jafino, “Flood exposure and poverty in 188 countries,” *Nat. Commun.*, vol. 13, no. 1, Dec. 2022, doi: 10.1038/s41467-022-30727-4.

[10] B. Merz, H. Kreibich, R. Schwarze, and A. Thieken, “Review article ‘assessment of economic flood damage,’” 2010. doi: 10.5194/nhess-10-1697-2010.

[11] B. Jongman *et al.*, “Declining vulnerability to river floods and the global benefits of adaptation,” *Proceedings of the National Academy of Sciences*, vol. 112, no. 18, May 2015, doi: 10.1073/pnas.1414439112.

[12] J. C. J. H. Aerts *et al.*, “Exploring the limits and gaps of flood adaptation,” *Nature Water*, vol. 2, no. 8, pp. 719–728, 2024, doi: 10.1038/s44221-024-00274-x.

[13] O. E. J. Wing *et al.*, “Inequitable patterns of US flood risk in the Anthropocene,” *Nat. Clim. Chang.*, vol. 12, no. 2, pp. 156–162, Feb. 2022, doi: 10.1038/s41558-021-01265-6.

[14] M. Tanoue, R. Taguchi, H. Alifu, and Y. Hirabayashi, “Residual flood damage under intensive adaptation,” *Nat. Clim. Chang.*, vol. 11, pp. 823–826, 2021, doi: 10.1038/s41558-021-01158-8.

[15] J. L. Kephart *et al.*, “Social disparities in neighborhood flood exposure in 44,698 urban neighborhoods in Latin America,” *Nature Cities*, vol. 2, no. 3, pp. 246–253, Feb. 2025, doi: 10.1038/s44284-025-00203-3.

[16] J. L. Stoddard, D. P. Larsen, C. P. Hawkins, R. K. Johnson, and R. H. Norris, “Setting expectations for the ecological condition of streams: The concept of reference condition,” 2006, *Ecological Society of America*. doi: 10.1890/1051-0761(2006)016[1267:SEFTEC]2.0.CO;2.

[17] C. P. Hawkins, J. R. Olson, and R. A. Hill, “The reference condition: predicting benchmarks for ecological and water-quality assessments,” *J. North Am. Benthol. Soc.*, vol. 29, no. 1, pp. 312–343, Mar. 2010, doi: 10.1899/09-092.1.

[18] R. D. Mazor *et al.*, “Bioassessment in complex environments: Designing an index for consistent meaning in different settings,” *Freshwater Science*, vol. 35, no. 1, pp. 249–271, Mar. 2016, doi: 10.1086/684130.

[19] H. Hämäläinen, J. Aroviita, J. Jyväsjärvi, and S. Kärkkäinen, “Dangerous relationships: biases in freshwater bioassessment based on observed to expected ratios,” *Ecological Applications*, vol. 28, no. 5, pp. 1260–1272, Jul. 2018, doi: 10.1002/eap.1725.

[20] A. S. Fotheringham and W. S. Wong, “The modifiable areal unit problem in multivariate statistical analysis,” 1991.

[21] H. Harintaka, A. G. Suhadha, A. Syetiawan, M. Ardha, and A. Rarasati, “Current land subsidence in Jakarta: a multi-track SBAS InSAR analysis during 2017–2022 using C-band SAR data,” *Geocarto Int.*, vol. 39, no. 1, 2024, doi: 10.1080/10106049.2024.2364726.

[22] L. Cea and P. Costabile, “Flood Risk in Urban Areas: Modelling, Management and Adaptation to Climate Change. A Review,” *Hydrology*, vol. 9, no. 3, p. 50, Mar. 2022, doi: 10.3390/hydrology9030050.

[23] J. Zhao, M. Li, Y. Li, P. Matgen, and M. Chini, “Urban Flood Mapping Using Satellite Synthetic Aperture Radar Data: A review of characteristics, approaches, and datasets,” 2025, *Institute of Electrical and Electronics Engineers Inc.* doi: 10.1109/MGRS.2024.3496075.

[24] W. G. Manning and J. Mullahy, “Estimating log models: to transform or not to transform?,” *J. Health Econ.*, vol. 20, no. 4, pp. 461–494, 2001, doi: https://doi.org/10.1016/S0167-6296(01)00086-8.

[25] J. M. C. Santos Silva and S. Tenreyro, “The log of gravity,” *Review of Economics and Statistics*, vol. 88, no. 4, pp. 641–658, Nov. 2006, doi: 10.1162/rest.88.4.641.

[26] P. K. Dunn and G. K. Smyth, “Series evaluation of Tweedie exponential dispersion model densities,” *Stat. Comput.*, vol. 15, no. 4, pp. 267–280, 2005, doi: 10.1007/s11222-005-4070-y.

[27] L. Anselin, “Local Indicators of Spatial Association—LISA,” *Geogr. Anal.*, vol. 27, no. 2, pp. 93–115, 1995, doi: 10.1111/j.1538-4632.1995.tb00338.x.

[28] Y. Benjamini and Y. Hochberg, “Controlling the False Discovery Rate: A Practical and Powerful Approach to Multiple Testing,” *Journal of the Royal Statistical Society. Series B (Methodological)*, vol. 57, no. 1, pp. 289–300, 1995, [Online]. Available: http://www.jstor.org/stable/2346101

[29] R. S. Bivand and D. W. S. Wong, “Comparing implementations of global and local indicators of spatial association,” *Test*, vol. 27, no. 3, pp. 716–748, Sep. 2018, doi: 10.1007/s11749-018-0599-x.

[30] C. F. Dormann *et al.*, “Methods to account for spatial autocorrelation in the analysis of species distributional data: A review,” Dec. 2007. doi: 10.1111/j.2007.0906-7590.05171.x.

[31] H. Kreibich *et al.*, “Adaptation to flood risk: Results of international paired flood event studies,” *Earths Future*, vol. 5, no. 10, pp. 953–965, Oct. 2017, doi: 10.1002/2017EF000606.

[32] H. Kreibich *et al.*, “How to improve attribution of changes in drought and flood impacts,” *Hydrological Sciences Journal*, vol. 64, no. 1, pp. 1–18, Jan. 2019, doi: 10.1080/02626667.2018.1558367.

[33] F. Yuan, Y. Yang, Q. Li, and A. Mostafavi, “Unraveling the Temporal Importance of Community-Scale Human Activity Features for Rapid Assessment of Flood Impacts,” *IEEE Access*, vol. 10, pp. 1138–1150, 2022, doi: 10.1109/ACCESS.2021.3137651.

[34] Changjie Chen *et al.*, “Integrating Urban Digital Twin with Cloud-Based Geospatial Dashboard for Coastal Resilience Planning: A Case Study in Florida,” *J. Plan. Educ. Res.*, vol. 45, no. 4, pp. 743–759, Dec. 2025, doi: 10.1177/0739456X251316185.

Supplementary Files

This is a list of supplementary files associated with this preprint. Click to download.

- HNFBDevSupplementaryInformation.docx